Vol. 92 No. 6 pp. 2201–2213 ACTA GEOLOGICA SINICA (English Edition) Dec. 2018

Iron Speciation of Mud Breccia from the Dushanzi Mud Volcano in the Xinjiang Uygur Autonomous Region, NW China

XU Wang[1, 2], ZHENG Guodong[1, *], MA Xiangxian[1], Danielle FORTIN[3], David R. HILTON[4], LIANG Shouyun[5], CHEN Zhi[6] and HU Guoyi[7]

1 *Key Laboratory of Petroleum Resources, Gansu Province / Key Laboratory of Petroleum Resources Research, Institute of Geology and Geophysics, Chinese Academy of Sciences, Lanzhou 730000, China*
2 *University of Chinese Academy of Sciences, Beijing 100049, China*
3 *Department of Earth and Environmental Sciences, University of Ottawa, 25 Templeton St., Ottawa, Ontario, K1N 6N5, Canada*
4 *Scripps Institution of Oceanography, University of California San Diego, La Jolla, CA 92093-0244, USA*
5 *Key Laboratory of Mechanics on Disaster and Environment in Western China (Lanzhou University), Ministry of Education, Lanzhou 730000, China*
6 *CEA Key Laboratory of Earthquake Prediction (Institute of Earthquake Forecasting), China Earthquake Administration, Beijing 100036, China*
7 *Research Institute of Petroleum Exploration and Development, PetroChina, Beijing 100083, China*

Abstract: Organic-inorganic interactions occurring in petroleum-related mud volcanoes can help predict the chemical processes that are responsible for methane emissions to the atmosphere. Seven samples of mud breccia directly ejected from one crater were collected in the Dushanzi mud volcano, along with one argillite sample of the original reddish host rocks distal from the crater, for comparison purposes. The mineral and chemical compositions as well as iron species of all samples were determined using XRD, XRF and Mössbauer spectroscopy, respectively. The results indicate that a series of marked reactions occurred in the mud volcano systems, more specifically in the mud breccia when compared to the original rocks. Changes mainly included: (1) some conversion of clay minerals from smectite into chlorite and illite, and the precipitation of secondary carbonate minerals such as calcite and siderite; (2) silicon depletion and significant elemental enrichment of iron, manganese, magnesium, calcium and phosphorus; and (3) transformation of iron from ferric species in hematite and smectite into ferrous species in siderite, chlorite and illite. These geochemical reactions likely induced the color changes of the original reddish Neogene argillite to the gray or black mud breccia, as a result of reduction of elements and/or alteration of minerals associated with the oxidation of hydrocarbons. Our results also suggest that greenhouse gases emitted from the mud volcanoes are lowered through a series of methane oxidation reactions and carbon fixation (i.e., through carbonate precipitation).

Key words: mud volcano, mud breccias, iron species, organic-inorganic interactions, greenhouse gas

1 Introduction

The environmental aspects of natural gas seepage from the Earth's surface have led to an increased interest due to its important role in global climate change. The surface seepage of natural gas containing methane, ethane and propane leads to the injection of these gases into the atmosphere (Etiope, 2015). Methane, as the third most important greenhouse gas after H_2O and CO_2, has a global warming potential that is 28 times higher than that of CO_2 on equal moles (Houghton et al., 2001). With the complement of seepage flux data and understanding of the role geological processes in the global methane budget, the geological methane seepage has been considered a major contributor to atmospheric methane concentrations (Etipoe and Klusman, 2002; Etiope, 2010). Total geological methane emissions are the second most important natural source of methane after wetlands, as recently outlined in the assessment reports of the IPCC in

* Corresponding author. E-mail: gdzhbj@mail.iggcas.ac.cn

2013 (Ciais et al., 2013). Mud volcanoes, as one of the most important geological sources of methane, are the largest surface expression of the migration of hydrocarbon fluids in petroleum bearing sedimentary basins (Dimitrov, 2002; Etiope, 2015). A wide array of scientific literature is available on the source of mud, water and gases released from mud volcanoes (You et al., 2004; Hensen et al., 2007; Nakada et al., 2011; Dai Jinxing et al., 2012; Li et al., 2014) and the methane fluxes from mud volcanoes to the atmosphere (Klusman et al., 2000; Etiope et al., 2004; Yang et al., 2004; Kopf et al., 2009; Hong et al, 2013; Zheng et al., 2017). However, there has been less attention and insufficient research on organic-inorganic interactions between hydrocarbons and inorganic minerals in mud volcano systems (Zheng et al., 2010). Organic-inorganic interactions occurring in mud volcanoes can help predict the chemical processes, which are most responsible for methane emissions to the atmosphere. The recognition of redox conditions is essential to explain organic-inorganic interactions between geofluids and the solid rocks (Zhu Dongya et al., 2017). Iron-bearing minerals exist widely in sediments and their speciation are quite useful to determine the redox conditions of sediments and/or rocks. Mössbauer spectroscopy is a powerful nuclear technique for characterizing the chemical states of iron. In this paper, we report on a series of variations in mineral compositions and iron speciation of the mud breccia directly overflowed from the Dushanzi mud volcano. We then compare our results with the original reddish host rocks, investigate the organic-inorganic interactions in the Dushanzi mud volcano system, and discuss their significance with respect to some related geological and geochemical implications.

2 Geological Setting

The Dushanzi mud volcano, located at the southern Dushanzi town in the Xinjiang Uygur Autonomous Region, NW China, is active with eruptions of crude oils, natural gases, formation water and even some mud breccia. The meaning of Dushanzi in Chinese for local people refers to a single hill or small mountain surrounded by the Gebi desert. This area is situated on the transition zone between the north-most front of the Tianshan Mountains to the south and the southern margin of the Junggar Basin to the north (Fig. 1a, b). The Junggar Basin is one of the largest Mesozoic-Cenozoic sedimentary basins in China, which is enriched in coals, asphalts, crude oils and natural gases (Li Jian et al., 2009; Chen Jianping et al., 2016). There are several rows of anticlines in the southern part of the Junggar Basin, which are geologically composed of three sub-parallel fold-and-thrust belts with structural deformations resulted from the northern thrusting of the Tiansshan Mountains (Avouac et al., 1993; Fu et al., 2003; Yang Geng et al., 2016). Those anticlines are normally dissymmetric in shape with the northern flank deeper and the southern flank relatively gentler. Some normal faults exist along the central axis of the Dushanzi anticline, providing suitable pathways for migration and eruption of hydrocarbons, water and mud. In fact, the present central Dushanzi anticline is a broken petroleum reservoir that has been unearthed along with uplifting and washing. Because of the uplift and erosion, the original oil reservoir is directly exposed to the surface, and some migration channels and/or networks for geo-fluids are still observed at present time.

Due to strong erosion and washing, the Dushanzi hill has been cut into many segments with numerous dry streams and/or small valleys. The color change of the same layer of sedimentary rocks on the slopes can be clearly observed ranging from reddish rocks far away to the central part of the Dushanzi anticline to yellowish and greenish rocks, where the Dushanzi mud volcano occurs (Fig. 2). These color changes for the same layer of rocks are mainly due to the bleaching effect by crude oils and natural gases along with the activity of former mud volcanoes (Fu et al., 2007; Zheng et al., 2010). The Dushanzi area has a typical inland arid climate with abundant sunshine, high evaporation, sparse vegetation and large diurnal fluctuations in air temperature: these conditions have induced strong physical weathering on surface rocks but less chemical weathering. Therefore, the Dushanzi area provides a suitable site for the geochemical study of the interactions between hydrocarbons and minerals, and the properties of petroleum reservoir rocks. Particularly, the gray to black fresh breccia erupted from the active mud volcano may supply useful information about the complex interactions underground.

Several mud volcano craters have developed on the Dushanzi hill. The crater DSZ-01 is a single isolated crater with a diameter of about 1.5 m, still erupting with crude oils, natural gases, water and mud during our field trips in April 2010, August 2014 and September 2016. Along with the eruption of fluids, mud was observed flowing out from the crater and continuously moving downward on the slope. The freshly erupted mud on the slope progressively dries while running its course, but the surface color remains deep gray or black. The mud breccia was very sticky when it was wet and semi-dried.

3 Samples and Analytical Method

Seven samples were collected from the mud breccia at different distance from the DSZ-01 crater (Fig. 1c). One reddish argillite sample, marked as rock-00, was also

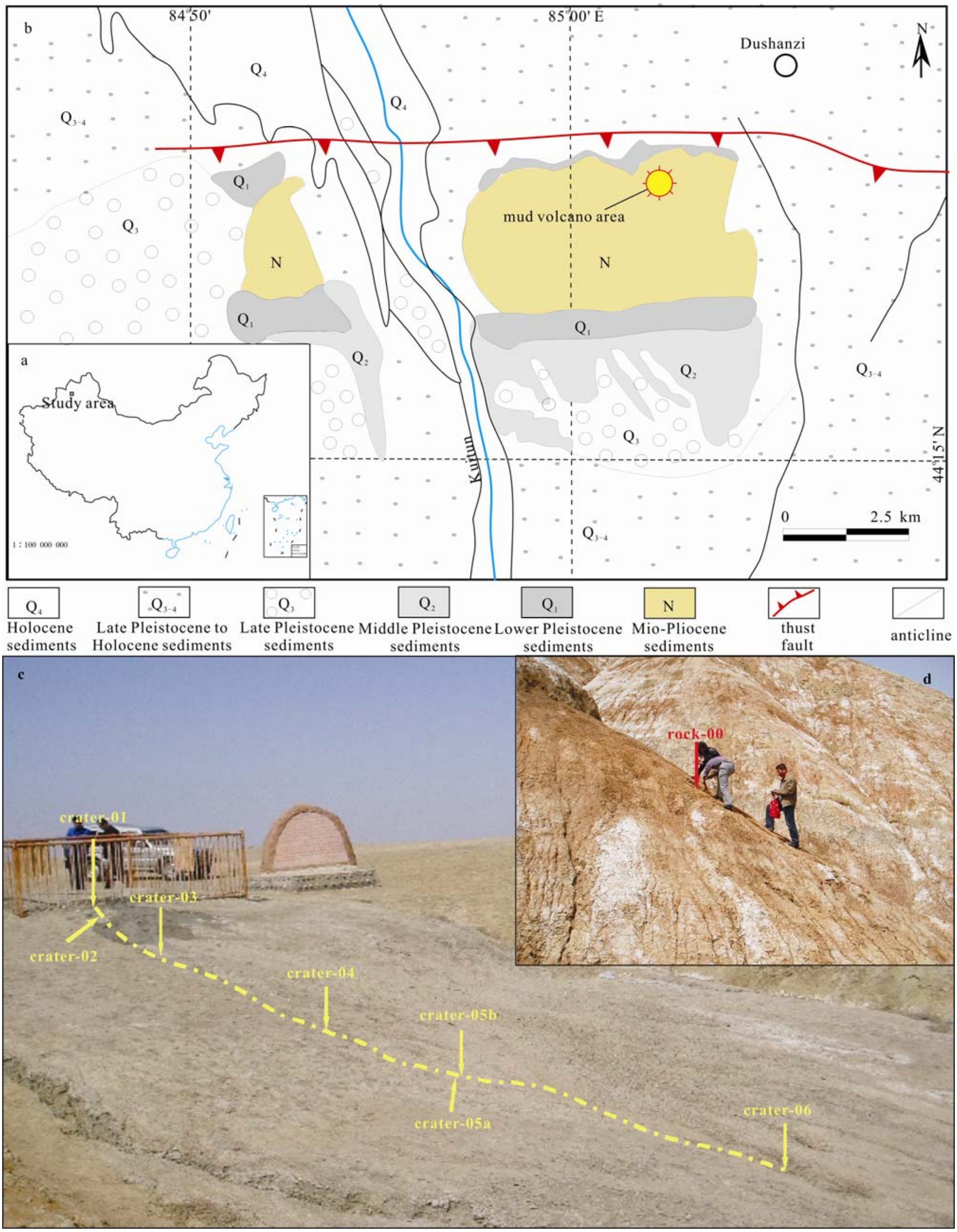

Fig. 1. Sketch map showing the geologic structure around the Dushanzi mud volcano and two photographs showing the erupting mud flow of the crater DSZ-01 and the host rocks of Mio-Pliocene sedimentary rocks(China basemap after China National Bureau of Surveying and Mapping Geographical Information).

(a), Small map showing the location of the study area; (b), geological map of Dushanzi District; (c), photograph showing the crater DSZ-01 and sampling locations; (d), photograph showing outcrop of host rocks and sampling location. China base-map after China National Bureau of Surveying and Mapping Geographical Information.

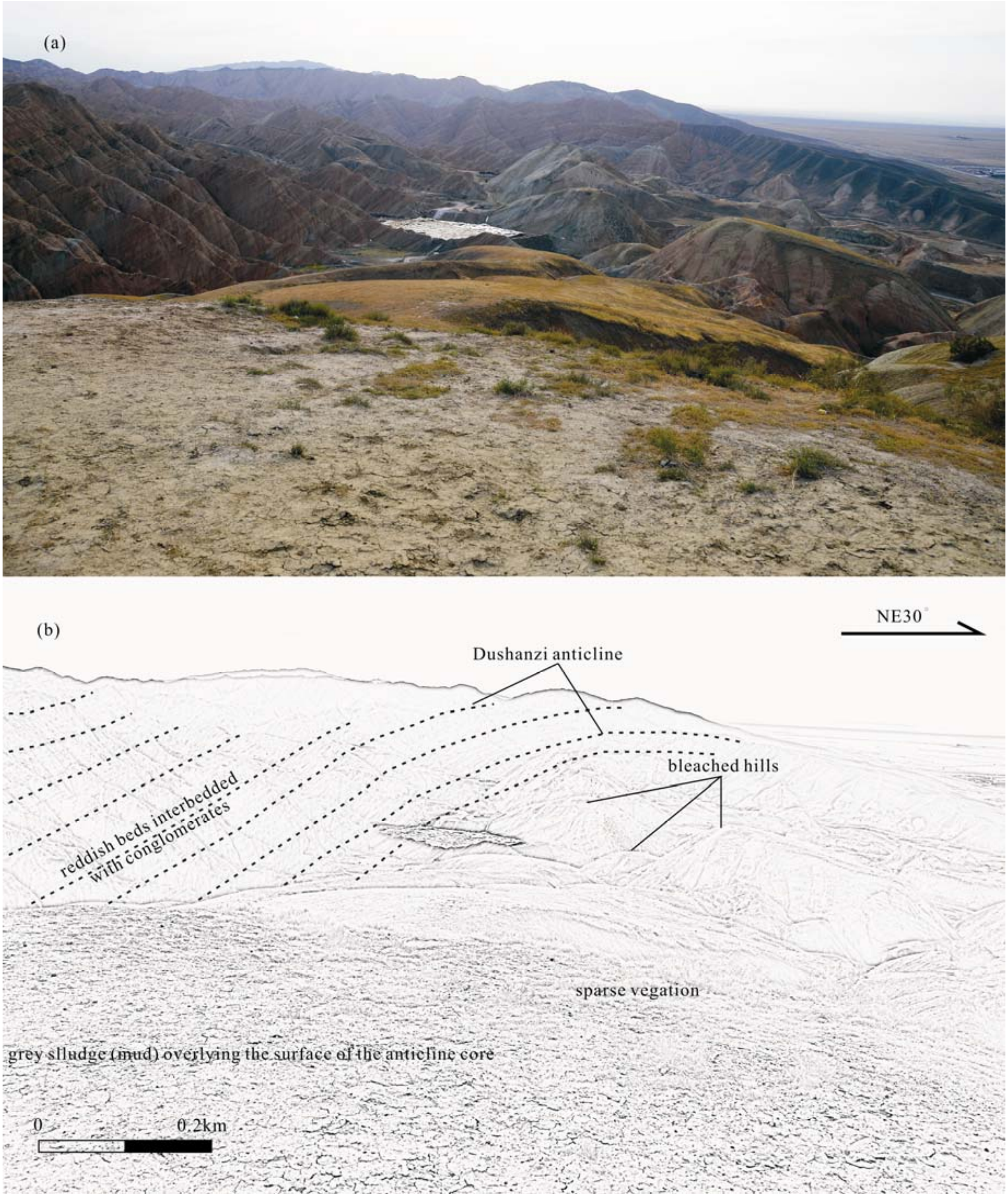

Fig. 2. Photograph (a) and sketch (b) showing the outcrop of the Dushanzi anticline and bleaching of the red beds.

collected from the original reddish Neogene sedimentary sequence distal from the mud volcano's crater but from the same Dushanzi anticline for comparison purposes (Fig. 1d). The characteristics of all the collected samples are shown in Table 1. The color of the sample powder is compared to the Revised Standard Soil Color Charts (Oyama and Takehara, 2002).

The wet mud breccia samples were freeze-dried and crushed into powder using an agate mortar and pestle. The argillite sample was also crushed into powder using the same tools. For the sake of avoiding contamination and minimize chemical variations of the original iron components, all samples were stored under dry and hermetic conditions. The sample powders were analyzed for mineral composition, major elemental contents and iron species with the help of X-ray diffraction, X-ray fluorescence spectrometry and Mössbauer spectroscopy, respectively. The mineral composition of the samples was

Table 1 General properties of Dushanzi mud volcano in the Xinjiang Autonomous Region, Northwestern China

Samples	Distance (m)	Color / Code	Notes
crater-01	Inner crater	Gray 10Y6/1	Mud breccia + Water, sampled with a 250 mL polyethylene plastic bottle
crater-02	Around crater	Yellowish gray 2.5Y5/1	Mud breccia (dry), saved with a 60 mL glass bottle
crater-03	2.8	Gray 5Y6/1	Mud breccia (wet), saved with a 60 mL glass bottle
crater-04	7.6	Yellowish gray 2.5Y5/1	Mud breccia (wet), saved with a 60 mL glass bottle
crater-05a	10.6	Yellowish gray 2.5Y6/1	Mud breccia (dry), saved with a 60 mL glass bottle
crater-05b	10.7	Gray 5Y6/1	Mud breccia (wet), saved with a 60 mL glass bottle
crater-06	17	Gray 5Y6/1	Mud breccia (wet), saved with a 60 mL glass bottle
rock-00	>1000	Red 7.5R4/8	Argillite (country rock), saved with seal sample bag

performed using a MAC Science M18XHF diffractometer fitted with a graphite monochromator. A wavelength-dispersive X-ray fluorescence spectrometer (Rigaku Co. ZSX-101e) operated at 50 kV and 50 mA was used to determine the chemical composition of major elements. A detailed description of the operating procedure can be found in Zheng et al. (2010). Loss on ignition (LOI) was determined by heating the bulk powder samples in an oven at 105°C for 2 h and then in a Muffle furnace at 850°C for 6 h (Zheng et al., 2004). About 250–350 mg of freshly powdered sample was gently pressed into a brass sample holder (16 mm in diameter, 1 mm thick) for ^{57}Fe Mössbauer spectroscopy analysis. The brass sample holder was closed at both ends with iron-free plastic tap. The Mössbauer spectra were acquired with an Austin Science S-600 Mössbauer spectrometer using a γ-ray source of 1.11 GBq ^{57}Co/Rh at a constant temperature of 293 K. The obtained spectra were fitted to Lorentzian line-shapes using standard line-shape fitting routines. Peak intensity and Half-width (HW) of each quadruple doublet was restricted to be equal. Isomer shifts (IS) were expressed with regard to the centroid of the spectrum of metallic iron foil (Kuno et al., 1998).

4 Results and Discussion

4.1 Variations of mineralogical composition

The X-ray diffraction results for all samples analyzed in this study are shown in Fig. 3. The mineral assemblage of most samples is primarily composed of quartz, albite, calcite, illite, chlorite, muscovite and smectite. These types of minerals are commonly found in the classic sedimentary rocks, for example, in the Mesozoic-Cenozoic reddish and green beds widely distributed in northwest China. However, there are clear distinguishable mineralogical compositions and relative content differences between the mud breccia samples and the argillite sample.

As illustrated in Fig. 3, chlorite, illite and muscovite were found in all samples, but their peak heights are relatively higher in the mud breccia compared to those in the sample rock-00. Smectite with a strong wide peak was

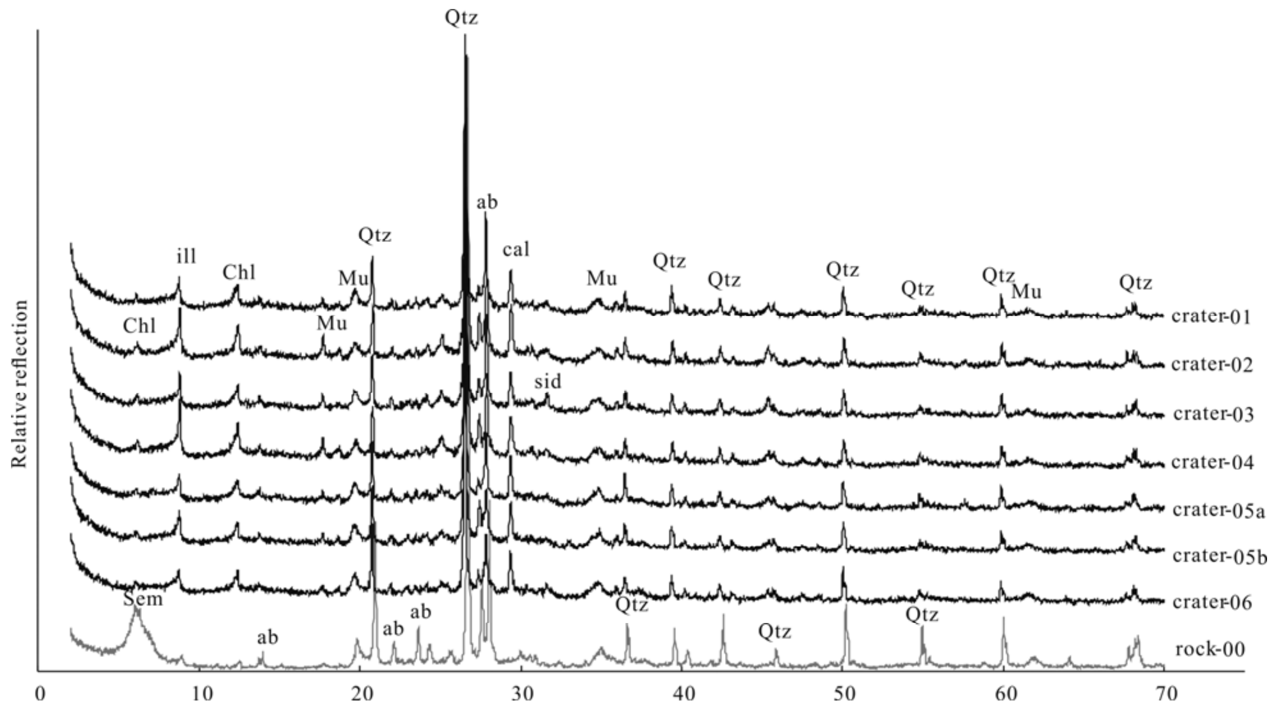

Fig. 3. X-ray diffraction patterns for the study samples.
Sm-smectite; Chl-chlorite; ill-illite; ab-albite; Mu-muscovite; Qtz-quartz; Cal-calcite; sid-siderite.

only identified in the sample rock-00. These different characteristics might indicate some conversion of clay minerals e.g., from smectite to chlorite and illite, that occurred in the mud volcano systems. Conventionally, the conversion of clay minerals requires an adequately high temperature. According to the equilibrium temperature calculated from the oxygen isotope fractionation between water and calcite of the Dushanzi mud volcano, the mean temperature of the water-rock interactions is approximately 81° C (Nakada et al., 2011). This temperature is enough for the dehydration of smectite and the conversion of smectite into illite (Pytte and Reynolds, 1989). In addition, the pH and Eh values of the sludgy liquid in the Dushanzi mud volcano system were within a range of 8.0 to 9.0 and −50 to −120 mV, respectively, as measured in-situ during many field investigations over the last 5 years. It is very likely that a weakly alkaline medium and reducing conditions played a key role in the conversion of some clay minerals.

As shown in Fig. 3, besides the main peak for quartz at 26.54°, there is a group of peaks (4–5 peaks) at 67.7°–69.1° (2θ) for all samples. This group of peaks represents typical diffraction peaks for quartz, and their relative heights were quite different among the study samples, especially between the mud breccia and the argillite sample, showing stronger peaks for the argillite sample and relatively weaker peaks for the mud breccia samples. Such differences likely indicate some variations in quartz crystal structures along with petroleum bleaching. The diffracting peaks of felsic minerals (quartz and albite) were relatively weaker in the mud breccia than that of the argillite sample, suggesting a relatively lower content of felsic minerals in the petroleum-bleached mud than that in the unbleached original argillite. One of the possible processes responsible for this could be some depletion of felsic minerals as petroleum fluids interacted with those minerals in the host rocks.

Several types of carbonate minerals were identified in the mud breccia whereas there were no clear peaks corresponding to carbonate minerals in the argillite sample. This difference may be explained by the precipitation of some carbonate minerals during the petroleum bleaching. The fluids in the crater DSZ-01 are weakly alkaline (pH=8.0–9.0). Under weakly alkaline medium, carbonate anions (HCO_3^- and CO_3^{2-}) can react with metal cations, such as calcium (Ca^{2+}), manganese (Mn^{2+}), magnesium (Mg^{2+}) and iron (Fe^{2+}) in solution (Li et al., 2014), and form secondary carbonate minerals that can precipitate as solid minerals, such as $CaCO_3$, $MnCO_3$, $MgCO_3$ and $FeCO_3$. In addition, the highest peak for siderite was observed in the sample crater-03 that was a fresh grey mud breccia with a strong gasoline smell. The formation of siderite is a strong evidence for the redox transformation of ferric iron to ferrous iron during petroleum bleaching.

4.2 Chemical compositions of major elements

The relative content of major elements and loss on ignition (LOI) of the bulk samples are presented in Table 2. There are distinct differences in major element contents between the mud breccia and the argillite sample. Furthermore, clear variations in major elements and LOI were also observed among the mud breccia collected from the same mud flow but at different distances from the active crater. A more detailed depiction of the variations of each major element for all samples is shown in Fig. 4.

As shown in Fig. 4 and Table 2, the silicon contents are sharply different between the mud breccia and the argillite sample, showing a decrease in SiO_2 contents from 72.8% in the argillite sample to 51.8%–57.2% in the mud breccia samples. These results agree well with the mineralogical composition determined by XRD, showing a clear decrease of felsic minerals, including quartz and albite, in the mud breccia compared to the argillite sample. The decrease in total silicon might indicate the dissolution of silicates along with petroleum bleaching (Zheng et al., 2010). In contrast, there was a marked increase in the relative contents of iron, manganese, magnesium and calcium in the mud breccia in comparison to argillite. All these elements are commonly found in carbonate minerals such as siderite and calcite in sedimentary rocks, which are considered as carbonate-forming elements. There was a positive correlation between the contents of carbonate minerals and the contents of these carbonate-forming elements (Table 2) in the mud samples, suggesting that these elements likely to be existed as secondary carbonates

Table 2 Relative content of the major elements and loss on ignition results of the samples

Samples	Relative content (wt%)											
	SiO_2	TiO_2	Al_2O_3	Fe_2O_3	MnO	MgO	CaO	Na_2O	K_2O	P_2O_5	LOI*	Total
crater-01	55.3	0.714	14.9	5.66	0.088	3.29	4.40	2.05	2.99	0.299	9.82	99.5
crater-02	55.1	0.701	14.7	5.58	0.089	3.37	4.58	2.09	2.98	0.319	9.68	99.2
crater-03	57.3	0.687	12.5	5.56	0.087	2.70	4.25	3.99	2.64	0.278	9.79	99.8
crater-04	55.5	0.702	14.7	5.64	0.087	3.13	4.34	2.25	2.97	0.320	8.40	98.0
crater-05a	51.8	0.681	14.0	5.50	0.085	3.03	4.16	7.61	2.84	0.309	8.76	98.8
crater-05b	55.5	0.708	14.8	5.61	0.087	3.31	4.42	2.13	2.99	0.318	9.91	99.8
crater-06	55.6	0.690	14.7	5.63	0.088	3.19	4.54	2.11	2.98	0.342	8.41	98.3
rock-00	72.8	0.622	13.9	3.39	0.058	1.75	1.26	2.18	2.74	0.104	3.24	102

*LOI means the weight loss during heating at temperature between 105 °C for 2 h and 850 °C for 6 h.

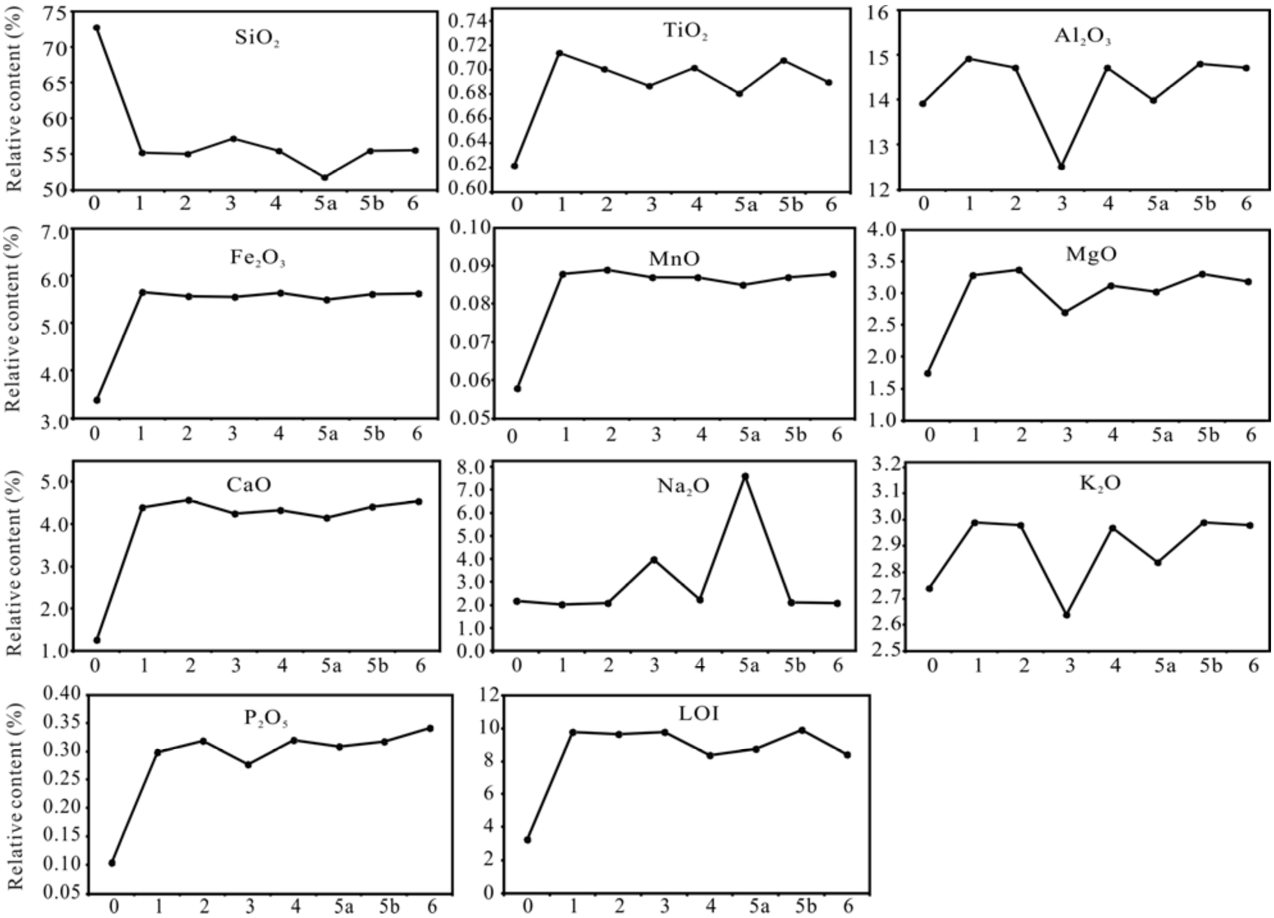

Fig. 4. Distribution of major elements and loss (wt%) on ignition (LOI) results for the study samples.

in the mud breccia. Phosphorous was also higher in the mud breccia than in the argillite sample. Previous studies have suggested that microbial activity can influence the phosphorous content of soils and rocks formed under natural conditions, particularly in the presence of iron oxides (Pikovskaya, 1948; Fortin et al., 2000; Zheng et al., 2007). Also, the variations of $\delta^{13}C_{CO2}$ show that oil biodegradation with CO_2 reduction likely occurs at a shallower depth along the seepage system of the mud volcano (Nakada et al., 2011). Thus, the enrichment of phosphorus in the erupted mud might be the contribution of biological processes within the mud volcanic systems. In addition, LOI values were clearly higher in the ejected mud breccia, probably indicating higher contents of organic matter or some other kinds of volatiles absorbed in the bleached muddy materials. The mixing of organic matter or some other kinds of fluids within the host rocks, likely caused the higher LOI values observed for the erupted mud breccia from the Dushanzi mud volcano.

4.3 Systemic variations of iron speciation

The ^{57}Fe Mössbauer spectra of all samples measured at room temperature (RT, constant around 293 K) are shown in Fig. 5, in which three doublets (D1, D2, D3) were observed in all samples whereas an additional sextet was only presented in the argillite sample. The curve fitting procedure for the iron components was robust, with sufficiently small Chi-squared values, indicating a reliable fitting. The corresponding iron species for all samples are listed in Table 3.

As shown in Fig. 5, the doublet (D1) with a smaller quadrupole splitting was ascribed to either paramagnetic high-spin ferric iron (para-Fe^{3+}) or iron sulfide, such as pyrite (pyr-Fe^{2+}). Previous studies have suggested that the para-Fe^{3+} presumably originated from clay minerals and/or hydrated ferric oxides (Manning and Ash, 1979). Therefore, it could be speculated that the para-Fe^{3+} in the mud breccia was most likely in the form of hydroxides. Based on Mössbauer parameters (Table 3) and the mineralogical compositions determined by XRD patterns (Fig. 3), the para-Fe^{3+} in sample rock-00 should be mainly due to ferric iron in hematite and smectite, whereas the para-Fe^{3+} in the mud breccia could be ferric iron in the remaining smectite or other clay minerals. The detection of pyrite can be difficult because of the small particle size, low content and dispersion within samples. In this study,

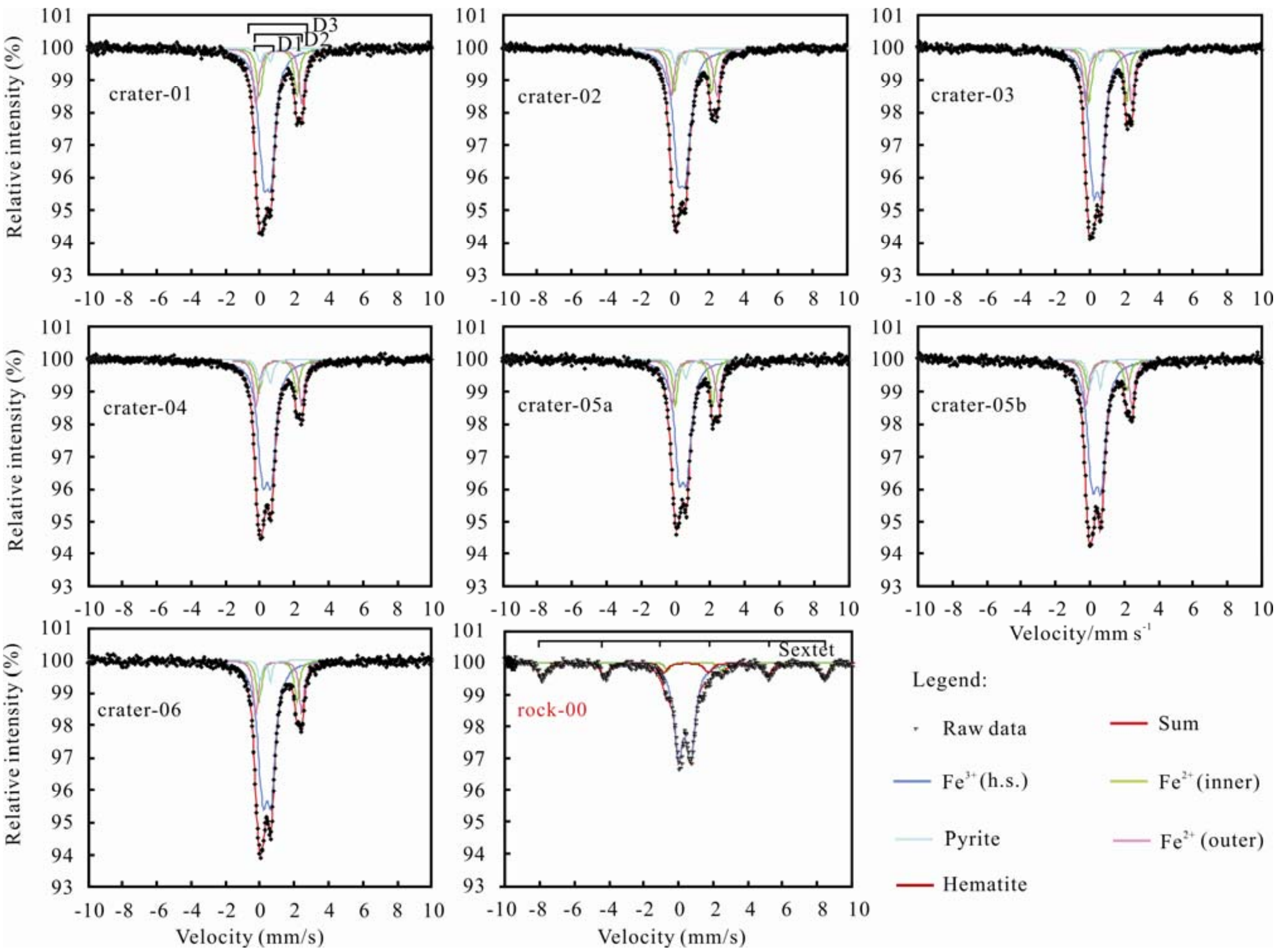

Fig. 5. Mössbauer spectra of study samples measured at room temperature (293 K). The upper indicator bars show the peak position of each iron species.

D1-doublet for ferrous iron in pyrite; D2-doublet for paramagnetic low-spin ferrous iron, para-Fe^{2+}(inner); D3-doublet for paramagnetic high-spin ferrous iron, para-Fe^{2+}(outer); Sextet for magnetic iron in hematite.

the pyr-Fe^{2+} was fitted with values of quadruple splitting (QS) 0.610 mm/s and isomer shift (IS) 0.307 mm/s for the Mössbauer spectra at 297 K. Pyrite was considered absent when the calculated peak area of pyr-Fe^{2+} was lower than the detection limit, and calculated as three times larger than the standard deviation of the baseline count (Kuno et al., 1998).

There were two doublets (D2, D3) with larger quadrupole splitting which appeared in the spectrum of the study samples. These two doublets were attributed to relatively paramagnetic low-spin or high-spin ferrous iron (para-Fe^{2+}), corresponding to two kinds of ferrous iron species as para-Fe^{2+} (inner) and para-Fe^{2+} (outer) in the mud breccia samples. According to these Mössbauer parameters, the para-Fe^{2+} (inner) with relatively lower IS, QS and HW may correspond to the ferrous iron in siderite or organic matter whereas the para-Fe^{2+} (outer) with relatively higher IS, QS and HW may represent the ferrous iron in clay minerals (Ram et al., 1998; Zachara et al., 2004; Medina et al., 2006). In a few cases, the ferrous iron in calcite and dolomite may display similar Mössbauer parameters as the ferrous iron in siderite due to their similar chemical structures and/or crystal structures (Ellwood et al., 1989).

As shown in Fig. 6, the relative content of ferric iron in the samples of mud breccia were all higher than that of the argillite sample (rock-00), clearly indicating some reducing conversion of ferric iron into ferrous iron from the original host rocks to the mud breccia. In addition, the relative content of ferric iron also varied among the mud breccia samples collected from different sampling points at different distances from the crater. The ratio of ferric vs. total iron ($Fe^{3+}/\Sigma Fe$) in the mud breccia (crater-02 – crater-06) was higher than that of the sludgy sample (crater-01), with a general increasing trend along with the increasing distance from the crater. This variation in $Fe^{3+}/\Sigma Fe$ ratios may indicate some conversion of ferrous iron to ferric iron after the mud erupted onto the ground surface and flowed away from the crater. After the ejected mud ran down on the ground surface, some dehydration and oxidation could

Table 3 Mössbauer parameters of the iron species in the samples (measured at 293 K)

Samples	Total peak area (%mm/s)	Species	Relative content (%)	I.S. (mm/s)	Q.S. (mm/s)	H.W. (mm/s)	Hi/T
crater-01	6.91±0.14	para-Fe^{3+}(h.s.)	60.43±0.71	0.423±0.006	0.445±0.009	0.643±0.013	
		para-Fe^{2+}(inner)	16.00±0.42	1.064±0.007	2.172±0.017	0.368±0.025	
		para-Fe^{2+}(outer)	20.07±0.44	1.120±0.004	2.675±0.015	0.400±0.018	
		pyr-Fe^{2+}	3.50±0.63	0.307±0.000	0.610±0.000	0.297±0.128	
crater-02	6.83±0.12	para-Fe^{3+}(h.s.)	62.72±0.58	0.419±0.004	0.465±0.007	0.691±0.013	
		para-Fe^{2+}(inner)	15.45±0.39	1.057±0.006	2.201±0.018	0.393±0.025	
		para-Fe^{2+}(outer)	18.01±0.39	1.120±0.005	2.666±0.016	0.419±0.019	
		pyr-Fe^{2+}	3.82±0.44	0.307±0.000	0.610±0.000	0.269±0.080	
crater-03	6.82±0.09	para-Fe^{3+}(h.s.)	61.55±0.45	0.419±0.004	0.454±0.005	0.593±0.007	
		para-Fe^{2+}(inner)	16.86±0.28	1.060±0.004	2.185±0.010	0.340±0.015	
		para-Fe^{2+}(outer)	18.51±0.27	1.113±0.003	2.678±0.010	0.362±0.012	
		pyr-Fe^{2+}	3.08±0.40	0.307±0.000	0.610±0.000	0.268±0.088	
crater-04	6.40±0.17	para-Fe^{3+}(h.s.)	62.76±0.86	0.408±0.007	0.513±0.006	0.650±0.011	
		para-Fe^{2+}(inner)	12.78±0.41	1.050±0.009	2.204±0.022	0.403±0.030	
		para-Fe^{2+}(outer)	17.37±0.43	1.116±0.004	2.660±0.013	0.385±0.017	
		pyr-Fe^{2+}	7.09±0.83	0.307±0.000	0.610±0.000	0.325±0.080	
crater-05a	6.54±0.18	para-Fe^{3+}(h.s.)	64.06±0.91	0.406±0.007	0.524±0.006	0.650±0.015	
		para-Fe^{2+}(inner)	12.03±0.50	1.047±0.012	2.225±0.031	0.413±0.043	
		para-Fe^{2+}(outer)	16.43±0.50	1.124±0.006	2.671±0.017	0.379±0.023	
		pyr-Fe^{2+}	7.48±0.81	0.307±0.000	0.610±0.000	0.290±0.073	
crater-05b	6.11±0.17	para-Fe^{3+}(h.s.)	60.68±0.92	0.415±0.007	0.466±0.009	0.628±0.012	
		para-Fe^{2+}(inner)	15.93±0.45	1.056±0.007	2.193±0.016	0.346±0.022	
		para-Fe^{2+}(outer)	17.38±0.45	1.114±0.004	2.694±0.014	0.373±0.019	
		pyr-Fe^{2+}	6.01±0.93	0.307±0.000	0.610±0.000	0.331±0.114	
crater-06	6.82±0.13	para-Fe^{3+}(h.s.)	65.08±0.63	0.404±0.005	0.498±0.006	0.626±0.012	
		para-Fe^{2+}(inner)	13.31±0.38	1.050±0.007	2.206±0.019	0.360±0.027	
		para-Fe^{2+}(outer)	17.18±0.38	1.115±0.004	2.668±0.013	0.359±0.017	
		pyr-Fe^{2+}	4.44±0.52	0.307±0.000	0.610±0.000	0.248±0.074	
rock-00	4.91±0.07	para-Fe^{3+}	67.93±0.61	0.347±0.004	0.707±0.006	0.626±0.011	
		para-Fe^{2+}	3.82±0.29	0.931±0.024	3.115±0.047	0.352±0.074	
		hem-Fe^{3+}	28.25±0.61	0.353±0.010	-0.199±0.020	0.557±0.038	50.41±0.08

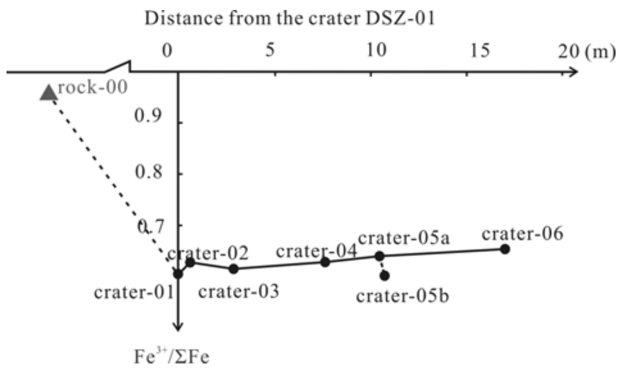

Fig. 6. Distribution of relative content of ferric iron vs. total iron with respect to distance from the active crater DSZ-01.

have taken place quickly due to the local arid climate. Such alteration would be reflected in the surface properties of the mud, such as the wetness and color changes. However, the samples of mud breccia all retained their reduced characteristics even after being exposed for some time on the ground surface. The samples crater-03 and crater-05b, characterized by grey and wet mud, had relatively less ferric irons than other mud breccia samples (crater-02, crater-04, crater-5a and crater-06). The sample crater-05b was taken from the subsurface of the sampling site of crater-05a. The relative content of ferrous iron in the sample crater-05b is relatively higher than that of crater-05a, being close to the value of the crater-01, suggesting the subsurface mud keeps similar characteristics of reducing iron species as does the sludgy mud. It should be noted that even though all mud breccia kept their gray colors without sharp differences, their iron species were distinguishably variable as shown by the Mössbauer results. This points to the importance of using Mössbauer spectroscopy over other techniques for such samples.

4.4 Organic-inorganic interactions in the mud volcano system

As shown in Fig. 7, the fresh grey sludge erupting from the crater and felling down on the slope of the mud cone. The fresh mud dries up rapidly and accumulate on the ground to form and expand the mud mount. This sludge originates from inside of the mud volcano system because no other sources of particulates such as air dust or sand from the desert were observed. The mud breccia is therefore a mixture of material from different strata or layers of rocks along the transportation pathways through faults and fractures under high pressure at depth. Based on the local geology, especially the tectonic and stratigraphic combination of the Dushanzi anticline, the mud breccia was probably derived mainly from the Neogene argillaceous, resembling thin layer of fine mudstone and/ or clay cement of the lacustrine classic rocks. The palynomorph records of the erupted mud suggest that the Cenozoic sedimentary rocks, mainly the Middle-Late Miocene Taxihe and Dushanzi Formations are the major

Fig. 7. Photograph showing the grey sludgy erupting from the Dushanzi mud volcano.

source for the mud breccia erupting from the Dushanzi mud volcano (Ji et al., 2017). Compared with the Neogene argillaceous rocks in the Dushanzi anticline and its surrounding areas, there were sharp characteristics changes in the erupted mud or sludge, which may indicate some systematical variations in mineral and chemical compositions of the ejected mud breccia from the original rocks and a series of organic-inorganic interactions occurring in the mud volcano systems.

On one hand, the variation in mineral composition from the original host rocks to the erupted mud may indicate some conversion of clay minerals such as smectite to chlorite and/or muscovite along with interactions between the solid rocks and certain geofluids, such as formation water, oils and gases during their migration. At the same time, the reducing and weakly alkaline medium should be favorable for the formation and precipitation of secondary carbonate minerals including calcite and siderite in the mud volcano system. These newly formed carbonate minerals and/or converted clay minerals would erupt along with the fluids to the ground surface, even mixed together with the fine particles of conglomerate in the host rocks. The local arid inland climate of the study area and the supply of snow-melt water from the Tianshan Mountains would therefore be essential to keep the environment under weakly alkaline medium suitable for the stability of secondary carbonate minerals within the mud volcano system (Zheng et al., 2010). In addition, pyrite was also precipitated under the reducing conditions. Those mineral variations caused a decrease of felsic minerals like quartz and albite (Fig. 3). Correspondingly, some major elements such as iron, manganese, magnesium and calcium were significantly increased while silicon was sharply decreased, being consistent with the mineral changes (Table 2). Because of the existence of reducing fluids maintained by crude oils and natural gases, the reduction of minerals and/or elements likely became the prominent processes in the mud volcano system. As a result, the reduction of ferric iron to ferrous iron and the conversion of smectite to chlorite have induced color changes from reddish hues of the original host rocks to deep gray or black of the bleached mud. These interactions can significantly modify the properties of the host rocks on the way of geo-fluids migration, such as their surface color (named as “Bleaching Effect” by Zheng et al., 2010), petrological structures and even some physical properties including porosity and permeability, which should be significant to the reconstruction of oil-gas reservoirs.

On the other hand, the geochemical properties of oil and gas were likely modified due to organic-inorganic interactions. Previous studies have demonstrated that the gases discharged from the Dushanzi mud volcano were predominantly thermogenic hydrocarbons (Nakada et al., 2011; Gao Yuan et al., 2012). The composition and isotopic characteristics of the gas from the Dushanzi mud volcano (DSZ-01) and Dushanzi well (Du-1) are shown in Table 4. The relative contents of CO_2 are 0.14% and 3.22% for the well gas from oil-gas well Du-1 and the emitted gas from the mud crater DSZ-01, respectively. Such variations indicate that the hydrocarbons (especially methane) from the reservoir were oxidized into carbon dioxide and other compounds during the migration of natural gases underground. In the Dushanzi mud volcano system, free oxygen is likely non-existent due to reducing condition indicated by the iron speciation and other geochemical indicators such as the oxidation-reduction potential (−54 mV) and conductivity (29.3 mS/cm). There was no oxygen detected in the gas samples from the Dushanzi mud volcanoes. The oxidized cations, such as ferric iron and manganese in the host rocks (e.g. conglomerate), would therefore act as electron acceptors in the absence of oxygen. The dissolved carbon dioxide could then be easily transformed into bicarbonate hydrogen ions and hydroxy radicals in the fluids under high subsurface pressures which maintain the formation waters under relatively alkaline conditions. These

Table 4 Composition and carbon isotopes of natural gas from the Dushanzi mud volcano and gas well

Sample ID	Gas composition (%)						$\delta^{13}C$ (‰, V-PDB)			
	CH_4	C_2H_6	C_3H_8	C_4H_{10}	C_5H_{12}	CO_2	CH_4	C_2H_6	C_3H_8	CO_2
DSZ-01	90.10	4.65	0.03	0.004	0.01	3.22	−41.4	−26.6	−10.1	+13.7
Du-1	79.74	9.27	3.42	1.56	0.52	0.14	−37.5	−27.1	−24.4	--

DSZ-01 is an active crater described in this study, the data refer to Gao Yuan et al. (2012); Du-1 is a well in the Dushanzi oilfield, the data refer to Sun Pingan et al. (2015).

processes have significant reference for the geological storage of carbon dioxide (Li Fucheng et al., 2016).

If methane from deep reservoirs was oxidized into carbon dioxide during its migration and then erupting to the atmosphere, the greenhouse effect would be decreased sharply, at least by a factor >20 times because the greenhouse effect of methane is about 28 times higher than that of equal moles of carbon dioxide (Houghton et al., 2001). The emitted gases from the Dushanzi mud volcano craters contain relatively high content of CO_2 when compare to the well gas from the oil-gas wells. Both the crater gas and the well gas were confirmed from the same petroleum reservoir (Sun Pingan et al., 2015), their original composition should be the same. Therefore, the variation in chemical composition between the crater gas and the well gas indicates some geochemical reactions within the mud volcano system. Furthermore, because of the existence of geological fluids including formation water in the mud volcano system, the carbon dioxide produced by oxidation of hydrocarbons could be easily dissolved in water and then combine with metal cations to form carbonate minerals and precipitate in solid phase. In this case, there should be no greenhouse gases emitted into the atmosphere, which might be considered as some kinds of carbon fixation in the mud volcano system. Altogether, there would be less carbon-containing gases erupted from mud volcano systems to the atmosphere compared with direct emission of natural gases from subsurface petroleum reservoirs. Such special geological processes could be called a “carbon fixation” process in mud volcano systems, which is simply summarized in Fig. 8.

5 Conclusions

Based on mineralogical and geochemical properties, as well as iron speciation of the erupted mud in comparison with the original fine argillite, some processes of organic-inorganic interactions were noted. Because of the existence of reducing fluids maintained by crude oils and natural gases, the reduction of minerals/elements and the oxidation of hydrocarbons occurred together and were the prominent processes in the Dushanzi mud volcano systems. As a result, the reduction of ferric iron to ferrous iron and the conversion of smectite to chlorite have induced color changes from the reddish hues of the original host rocks to deep gray or black of the erupted mud. The reducing and weakly alkaline medium contributed to the precipitation of secondary carbonate minerals including calcite and siderite, which may change the physical properties of the host rocks. The oxidation of methane and other hydrocarbons along with the precipitation of secondary carbonate minerals likely reduces greenhouse gas emissions, such as methane and lower CO_2 emissions mineral fixation.

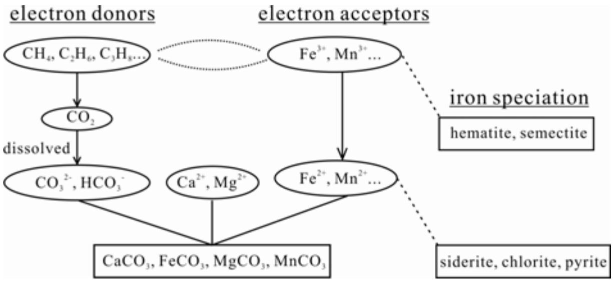

Fig. 8. Simplified flow-process diagram of organic-inorganic interactions between hydrocarbons and inorganic elements in the Dushanzi mud volcano system.

Acknowledgements

We would like to thank Prof. Bihong Fu and Prof. Zhengfu Guo for their discussion and comments on this study, Dr. Wenxiu Yu and Mr. Tao Liu for their help with fieldwork. This work was partially supported by the National Science and Technology Major Project of the Ministry of Science and Technology of China (2016ZX05007001-004), the National Natural Science Foundation of China (41273112; 41402129; 41020124002; 41402298), CAS "Light of West China" Program and Chinese Academy of Sciences Visiting Professorship for Senior International Scientists (2015VEA032).

Manuscript received Apr. 1, 2018
accepted Jun. 5, 2018
edited by Fei Hongcai

References

Avouac, J.P., Tapponnier, P., Bai, M., Hou, Y., and Wang, G., 1993. Active thrusting and folding along the northeastern Tianshan, and rotation of Tarim relative to Dzungaria and Kazakahstan. *Journal of Geophysical Research*, 8(B4): 6755–6804.

Chen Jianping, Wang Xulong, Deng Chunping, Liang Digang, Zhang Yueqian, Zhao Zhe, Ni Yunyan, Zhi Dongming, Yang Haibo and Wang Yutao, 2016. Oil and gas source, occurrence and petroleum system in the Junggar Basin, northwest China. *Acta Geologica Sinica*, 90(3): 421–450 (in Chinese with English abstract).

Ciais, P., Sabine, C., Bala, G., Bopp, L., Brovkin, V., Canadell, J., Chhabra, A., DeFries, R., Galloway, J., Heimann, M., Jones, C., Myneni, R.B., Piao, S., and Thornton, P., 2013. Carbon and other biogeochemical cycles. In: Stocker, T.F., (eds) Climate Change 2013: Physical Science Basis. *Contribution of Working Group I to the Fifth Assessment Report of IPCC*, Cambridge University Press, 465–570.

Dai Jinxing, Wu Xiaoqi, Ni Yunyan, Wang Zecheng, Zhao Changyi, Wang Zhaoyun and Liu Guixia, 2012. Geochemical characteristics of natural gas from mud volcanoes in the southern Junggar Basin. *Science China Earth Sciences*, 55(3): 355–367.

Dimitrov, L.I., 2002. Mud volcanoes: the most important pathway for degassing deeply buried sediments. *Earth-Science Reviews*, 59: 49–76.

Ellwood, B.B., Burkart, B., Rajeshwar, K., Darwin, R.L., Neeley, R.A., McCall, A.B., Long, G.J., Buhl, M.L., and Hickcox, C.W., 1989. Are the iron carbonate minerals, ankerite and ferroan dolomite, like siderite, important in paleomagnetism? *Journal of Geophysical Research: Solid Earth*, 94(B6): 7321–7331.

Etiope, G., 2010. Geological methane. In: Reay, D., Smith, P., and van Amstel, A. (eds.), *Methane and Climate Change*. Earthscan, London, 50-69.

Etiope, G., 2015. *Natural Gas Seepage: The Earth's Hydrocarbon Degassing*. Springer, 197.

Etiope, G., and Klusman, R.W., 2002. Geologic emissions of methane to the atmosphere. *Chemosphere*, 49: 777–789.

Etiope, G., Feyzullayev, A., Baciu, C., and Milkov, A.V., 2004. Methane emission from mud volcanoes in eastern Azerbaijan. *Geology*, 32: 465–468.

Etiope, G., Feyzullayev, A., and Baciu, C.L., 2009. Terrestrial methane seeps and mud volcanoes: A global perspective of gas origin. *Marine and Petroleum Geology*, 26(3): 333–344.

Fortin, D., Goulet, R., and Roy, M., 2000. The effect of seasonal variations of sulfate-reducing bacteria populations on Fe and S cycling in a constructed wetland. *Geomicrobilolgy Journal*, 17: 221–235.

Fu, B.H., Lin, A., Kano, K., Maruyama, T., and Guo, J., 2003. Quaternary folding in the eastern Tian Shan, northwestern China. *Tectonophysics*, 369(1): 79–101.

Fu, B.H., Zheng, G.D., Ninomiya, Y., Wang, C.Y., and Sun, G.Q., 2007. Mapping hydrocarbon induced mineralogical alteration in the northern Tian Shan using ASTER multispectral data. *Terra Nova*, 19(4): 225–231.

Gao Yuan, Wang Yongli, Zheng Guodong, Meng Pei, Wu Yingqin, Yang Hui, Zhang Hong and Wang Youxiao, 2012. Geochemical characteristics of natural gas from Dushanzi mud volcano in the Junggar Basin, Xinjiang. *Acta Geoscientica Sinica*, 33(6): 989–994. (in Chinese with English abstract)

Hensen, C., Nuzzo, M., Hornibrook, E., Pinherio, L.M., Bock, B., Magalhaes, V.H., and Bruckmann, W., 2007. Sources of mud volcano fluids in the Gulf of Cadizindications for hydrothermal imprint. *Geochimica et Cosmochimica Acta*, 71: 1232–1248.

Hong, W.L., Etiope, G., Yang, T.F., and Yu, C.P., 2013. Methane flux from miniseepage in mud volcanoes of SW Taiwan: comparison with the data from Italy, Romania, and Azerbaijan. *Journal of Asian Earth Science*, 65: 3–12.

Houghton, J.T., Ding, Y., Griggs, D.J., and Noguer, M., 2011. Climate Change 2001: The Scientific Basis Contribution of Working Group I to the Third Assessment Report of Intergovernmental Panel of Climate Change (IPCC). Cambridge: Cambridge University Press.

Ji, L.M., Zhang, M.Z., Ma, X.X., Xu, W., and Zheng, G.D., 2017. Characteristics of mixed sporopollen assemblage from sediments of Dushanzi mud volcano in southern Junggar Basin and indication to the source of mud and debris ejecta. *Marine and Petroleum Geology*, 89(1): 194–201.

Klusman, R.W., Leopold, M.E., and LeRoy, M.P., 2000. Seasonal variation in methane fluxes from sedimentary basins to the atmosphere: results from chamber measurements and modeling of transport from deep sources. *Journal Geophysical Research*, 105D: 24661–24670.

Kopf, A., Delisle, G., Faber, E., Panahi, B., Aliyev, C.S., and Guliyev, I., 2009. Long-term in situ monitoring at Dashgil mud volcano, Azerbaijan: a link between seismicity, pore-pressure transients and methane emission. *International Journal of Earth Sciences*, 99: 227–240.

Kuno, A., Matsuo, M., and Takano, B., 1998. Mössbauer spectroscopic study on vertical distribution of iron components in estuarine sediments collected from Tama River in Tokyo. *Hyperfine Interactions*, C3: 328–331.

Li Fucheng, Zhang Yang, Jia Xiaofeng, Li Xufeng, Jia Xiaoleng and Guo Shenxiu, 2016. A method for evaluating the suitability of CO_2 geological storage in deep saline aquifers. *Acta Geologica Sinica* (English Edition), 90(5): 1838–1851.

Li Jian, Jiang Zhenglong, Luo Xia, Wang Dongliang and Han Zhongxi, 2009. Geochemical characteristics of coal-measure source rocks and coal-derived gas in Junggar Basin, NW China. *Petroleum Exploration and Development*, 36(3): 365–374.

Li, N., Huang, H., and Chen, D., 2014. Fluid sources and chemical processes inferred from geochemistry of pore fluids and sediments of mud volcanoes in the southern margin of the Junggar Basin, Xinjiang, northwestern China. *Applied geochemistry*, 46: 1–9.

Manning, P., and Ash, L., 1979. Mössbauer spectral studies of pyrite, ferric and high-spin ferrous distributions in sulfide-rich sediments from Moira Lake, Ontario. *Canadian Mineralogist*, 17: 111–115.

Medina, G., Tabares, J.A., Pérez Alcázar, G.A., and Barraza, J.M., 2006. A methodology to evaluate coal ash content using siderite Mössbauer spectral area. *Fuel*, 85(5): 871–873.

Nakada, R., Takahashi, Y., Tsunogai, U., Zheng, G.D., and Shimizu, H., 2011. A geochemical study on mud volcanoes in the Junggar Basin, China. *Applied Geochemistry*, 26(7): 1065–1076.

Oyama, M., and Takehara, H., 2002. Standard Soil Color Charts, Fujihira Industry Co., Ltd.

Pytte, A.M., and Reynolds, R.C., 1989. The thermal transformation of smectite to illite. In Thermal history of sedimentary basins. Springer New York, 133–140.

Pikovskaya, R.I., 1948. Mobilization of phosphorus in soil in connection with vital activity of some microbial species. *Mikrobiologiya*, 17(362): 362–370.

Ram, S., Patel, K.R., Sharma, S.K., and Tripathi, R.P., 1998. Distribution of iron in siderite in sub-surface sediments of Jaisalmer Basin (India) using Mössbauer spectroscopy. *Fuel*, 77(13): 1507–1512.

Sun Pingan, Bian Baoli, Yuan Yunfeng, Zhang Xingya and Cao Jian, 2015. Natural gas in southern Junggar Basin in northwest China: Geochemistry and origin. *Geochimica*, 44(3): 275–288 (in Chinese with English abstract).

Yang Geng, Zhao Mengjun, Chen Zhuxin and Wang Xiaobo, 2016. Geometric evidence for several synchronous thrust faulting activities of the thrust belt in the southern margin of Junggar, North Tianshan. *Acta Geologica Sinica*, 90(4): 639–652 (in Chinese with English abstract).

Yang, T.F., Yeh, G.H., Fu, C.C., Wang, C.C., Lan, T.F., Lee, H.F., Chen, C.H., Walia, V., and Sung, Q.C., 2004.

Composition and exhalation flux of gases from mud volcanoes in Taiwan. *Environmental Geology*, 46: 1003–1011.

You, C., Gieskes, J.M., Lee, T., Yui, T., Chen, H., 2004. Geochemistry of mud volcano fluids in the Taiwan accretionary prism. *Applied Geochemistry*, 19: 695–707.

Zachara, J.M., Kukkadapu, R.K., Gassman, P.L., Dohnalkova, A., Fredrickson, J.K., and Anderson, T., 2004. Biogeochemical transformation of Fe minerals in a petroleum-contaminated aquifer. *Geochimica et Cosmochimica Acta*, 68 (8): 1791–1805.

Zheng, G.D., Fu, B.H., Duan, Y., Wang, O., Matsuo, M., and Takano, B., 2004. Iron speciation related to color of Jurassic sedimentary rocks in Turpan Basin, northwest China. *Journal of Radioanalytical and Nuclear Chemistry*, 261(2): 421–427.

Zheng, G.D., Lang, Y.H., Miyahara, M., Nozaki, T., and Haruaki, T., 2007. Iron oxide precipitate in seepage of groundwater from a landslide slip zone. *Environmental Geology*, 51(8): 1455–1464.

Zheng, G.D., Fu, B.H., Takahashi, Y., Kuno, A., Matsuo, M., and Zhang, J.D., 2010. Chemical speciation of redox sensitive elements during hydrocarbon leaching in the Junggar Basin, Northwest China. *Journal of Asian Earth Sciences*, 39(6): 713–723.

Zheng, G.D., Ma, X.X., Guo, Z.F., Hilton, R.D., Xu, W., Liang, S.Y., Fan, Q.H., and Chen, W.X., 2017. Gas geochemistry and methane emission from Dushanzi mud volcanoes in the southern Junggar Basin, NW China. *Journal of Asian Earth Sciences*, 149: 184–190.

Zhu Dongya, Liu Quanyou, Jin Zhijun, Meng Qingqiang and Hu Wenxuan, 2017. Effects of deep fluids on hydrocarbon generation and accumulation in Chinese petroliferous basins. *Acta Geologica Sinica* (English Edition), 91(1): 301–319.

About the first author

XU Wang, male; born in 1990 in Tianshui City, Gansu Province; doctor; graduated from China University of Geosciences in Beijing; a Ph.D candidate of the Northwest Institute of Eco-Environment and Resource, Chinese Academy of Sciences. He is now interested in study on geochemistry of petroleum reservoir rocks, gas emission and oil-gas-water-rock interactions (organic-inorganic interactions) in mud volcano systems, gas geochemistry of fault zones and hot springs. Email: xuwang14@mails.ucas.ac.cn (1571637453@qq.com); phone: 18719799283.